J Sci Comput (2018) 77:1605–1620
https://doi.org/10.1007/s10915-018-0691-0

A Strongly Conservative Hybrid DG/Mixed FEM for the Coupling of Stokes and Darcy Flow

Guosheng Fu[1] · **Christoph Lehrenfeld**[2]

Received: 8 December 2017 / Revised: 23 February 2018 / Accepted: 1 March 2018 /
Published online: 9 March 2018

Abstract We consider the coupling of free and porous media flow governed by Stokes and Darcy equations with the Beavers–Joseph–Saffman interface condition. This model is discretized using a divergence-conforming finite element for the velocities in the whole domain. Hybrid discontinuous Galerkin techniques and mixed methods are used in the Stokes and Darcy subdomains, respectively. The discretization achieves mass conservation in the sense of $H(\text{div}, \Omega)$, and we obtain optimal velocity convergence. Numerical results are presented to validate the theoretical findings.

Keywords HDG · Stokes–Darcy · Divergence-conforming · Beavers–Joseph–Saffman

Mathematics Subject Classification 65N30 · 65N12 · 76S05 · 76D07

1 Introduction

The construction of new finite element methods for the Stokes–Darcy coupled problem, in which the respective interface conditions are given by mass conservation, balance of normal forces, and the Beavers–Joseph–Saffman law, is a very active research area; see [1,3,4,7,8,12–14,16–18,20–22,31–33,37,39] and the references therein. These problems have many important applications such as the modeling of groundwater contamination through streams and filtration problems [27,28].

Dedicated to the 60th birthday of Professor Bernardo Cockburn.

✉ Guosheng Fu
Guosheng_Fu@brown.edu

Christoph Lehrenfeld
lehrenfeld@math.uni-goettingen.de

1 Division of Applied Mathematics, Brown University, 182 George St, Providence, RI 02912, USA

2 Institut für Numerische und Angewandte Mathematik, Lotzestr. 16-18, 37083 Göttingen, Germany

Fig. 1 Sketch of Darcy and Stokes domains and boundaries

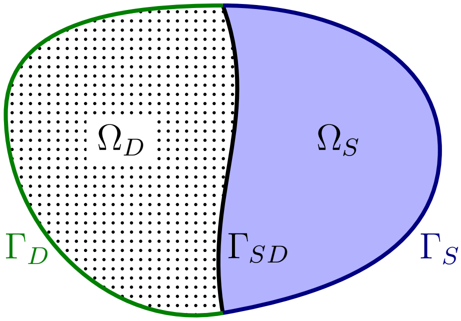

Among the methods cited above, Kanschat and Riviére [21] proposed a strongly conservative finite element method, where the Darcy flow is discretized by a mixed finite element method and Stokes flow by a mixed (velocity–pressure) discontinuous Galerkin (DG) method using a globally divergence-conforming velocity space on the whole domain. Such a method has the advantage that mass conservation is achieved in the sense of $H(\text{div}; \Omega)$, hence the name strongly conservative. Optimal error estimates of the method were proven in [20].

The divergence-conforming hybrid DG (HDG) method [9,15,24,25] for the Stokes flow is an efficient variant of the divergence-conforming DG method [11]. Due to hybridization, the HDG method has significant less globally coupled degrees of freedom, and has a better sparsity pattern than the DG method to achieve the same accuracy; see [25, Table 2] for a comparison.

In this paper, we present a strongly conservative HDG/mixed method for the Stokes-Darcy coupled problem by replacing the divergence-conforming DG method in the Stokes region with a divergence-conforming HDG method. Optimal error estimates of the method are proven. We maintain the advantage of mass conservation in terms of $H(\text{div}; \Omega)$, and have a reduced globally coupled degrees of freedom than the degrees of freedom for the method [21].

The rest of the paper is organized as follows. In Sect. 2, we first introduce the model problem then present our numerical method and show its wellposedness. In Sect. 3, we prove our main results on the optimal velocity error estimates. In Sect. 4, numerical results are presented to validate the theoretical findings. Finally, we conclude in Sect. 5.

2 Model Problem and Discretization

2.1 Model Problem

Let Ω be a bounded polygonal/polyhedral domain in $\mathbb{R}^d$, $d = 2, 3$, split into two polygonal/polyhedral subdomains Ω_S and Ω_D of free and porous media flow, respectively. Denote by Γ_{SD} the polygonal interface between Ω_S and Ω_D, cf. Fig. 1. The external boundaries are defined by

$$\Gamma_S = \partial\Omega \cap \partial\Omega_S, \quad \Gamma_D = \partial\Omega \cap \partial\Omega_D.$$

The coupled Darcy/Stokes problem in conservative form reads

$$-\nabla\cdot(2\nu\,\varepsilon(\boldsymbol{u})) + \nabla p = \boldsymbol{f}_S, \qquad \text{in } \Omega_S, \tag{1a}$$

$$K^{-1}\boldsymbol{u} + \nabla p = \boldsymbol{0}, \qquad \text{in } \Omega_D, \tag{1b}$$

$$\nabla\cdot\boldsymbol{u} = f_D\,\chi_{\Omega_D}, \qquad \text{in } \Omega. \tag{1c}$$

Here $\boldsymbol{u}$ is the velocity and p is the pressure. The deformation tensor is $\varepsilon(\boldsymbol{u}) = \frac{1}{2}(\nabla u+(\nabla u)^T)$, the coefficient $\nu > 0$ is the fluid kinematic viscosity, the variable $K > 0$ is ratio of the intrinsic permeability tensor to the fluid viscosity, which is symmetric and positive definite, and the function $\boldsymbol{f}_S$ is a body force in Stokes region, and f_D models source or sink in the porous medium. Whenever we want to distinguish between the solution of the Stokes and the Darcy subproblem, we refer to $\boldsymbol{u}_S = \boldsymbol{u}|_{\Omega_S}$ and $\boldsymbol{u}_D = \boldsymbol{u}|_{\Omega_D}$ and analogously for the pressures p_S and p_D. On the interface Γ_{SD}, this notation refers to the traces taken from the respective subdomains.

On the interface, we impose the Beavers–Joseph–Saffman conditions (see Beavers and Joseph [2] and Saffman [34]), and on the boundary, we assume no-slip and Neumann for simplicity:

$$\boldsymbol{u}_S\cdot\boldsymbol{n} = \boldsymbol{u}_D\cdot\boldsymbol{n}, \qquad \text{on } \Gamma_{SD}, \tag{2a}$$

$$p_S - 2\nu\varepsilon(\boldsymbol{u}_S)\boldsymbol{n}\cdot\boldsymbol{n} = p_D, \qquad \text{on } \Gamma_{SD}, \tag{2b}$$

$$\gamma\,K^{-1/2}(\boldsymbol{u}_S)^t + 2\nu(\varepsilon(\boldsymbol{u}_S)\boldsymbol{n})^t = 0, \qquad \text{on } \Gamma_{SD}, \tag{2c}$$

$$\boldsymbol{u}_S = \boldsymbol{0}, \qquad \text{on } \Gamma_S, \tag{2d}$$

$$\boldsymbol{u}_D\cdot\boldsymbol{n} = 0, \qquad \text{on } \Gamma_D. \tag{2e}$$

Here, $\gamma > 0$ is the phenomenological friction coefficient. On the interface Γ_{SD}, $\boldsymbol{n}$ is the unit normal vector pointing outward of Ω_S, and, on Γ_D, $\boldsymbol{n}$ is the unit normal vector pointing outward of Ω_D. The tangential component $(\cdot)^t$ of a vector $\boldsymbol{v}$ is denoted by $(\boldsymbol{v})^t = \boldsymbol{v}-(\boldsymbol{v}\cdot\boldsymbol{n})\boldsymbol{n}$.

2.2 Discretization

2.2.1 Preliminaries

Let $\mathcal{T}_h$ be a conforming simplicial triangulation of Ω such that the interface Γ_{SD} is the union of element facets. For any element $T \in \mathcal{T}_h$, we denote by h_T its diameter and we denote by h the maximum diameter over all mesh elements. Denote by $\mathcal{T}_{h,S}$ the set of mesh elements that belong to Ω_S and by $\mathcal{T}_{h,D}$ those belong to Ω_D. Denote by $\mathcal{F}_h$ the set of facets of $\mathcal{T}_h$, by $\mathcal{F}_{h,S}$ the set of facets that are interior to $\overline{\Omega_S}$, and by $\mathcal{F}_{h,SD}$ the set of facets that lie on the interface Γ_{SD}. We also denote by $\Gamma_{h,S}$ the set of facets that lie on the boundary Γ_S.

In the sequel, for the approximation of viscous forces in the Stokes region, we distinguish functions with support only on facets indicated by a subscript F and those with support also on the volume elements which is indicated by a subscript T. Compositions of both types are used for the HDG discretization of the velocity and indicated by underlining, $\underline{\boldsymbol{u}} = (\boldsymbol{u}_T, \boldsymbol{u}_F)$.

2.2.2 Finite Elements

We use the following stable pair of divergence-conforming velocity space $\boldsymbol{\Sigma}_h \subset H_0(\text{div},\Omega) = \{\boldsymbol{v} \in H(\text{div},\Omega) : \boldsymbol{v}\cdot\boldsymbol{n}|_{\partial\Omega} = 0\}$ and the matching pressure space

$Q_h \subset L^2_0(\Omega) = \{q \in L^2(\Omega) : \int_\Omega q \, \mathrm{dx} = 0\}$:

$$\boldsymbol{\Sigma}_h := \left\{ \boldsymbol{v}_T \in \prod_{T \in \mathcal{T}_h} [\mathbb{P}^k(T)]^d, \;\; [\![\boldsymbol{v}_T \cdot \boldsymbol{n}]\!]_F = 0 \, \forall F \in \mathcal{F}_h. \right\} \subset H_0(\mathrm{div}, \Omega), \tag{3a}$$

$$Q_h := \left(\prod_{T \in \mathcal{T}_h} \mathbb{P}^{k-1}(T) \right) \cap L^2_0(\Omega), \tag{3b}$$

where $[\![\cdot]\!]$ is the usual jump operator and $\mathbb{P}^k$ the space of polynomials up to degree k for $k \geq 1$. The Stokes operator is discretized by a divergence-conforming HDG method [25]. The benefits of divergence-conforming finite element discretizations for Stokes (or Navier–Stokes) problems is manifold. On the one hand divergence-conforming discretizations lead to solenoidal discrete solutions which can be crucial to obtain energy-stable discretizations for Navier–Stokes simulations, cf. [10]. On the other hand, already for Stokes problems the compatible treatment of the divergence-constraint is important to obtain *pressure*-robustness, i.e. a numerical scheme where the velocity error does not depend on the regularity of the pressure, cf. [26] and Theorems 1, 2 and 3 below. For a more detailed discussion of the benefit of divergence-conforming methods, we also refer to [36].

Divergence-conforming DG discretizations for Stokes (or Navier–Stokes) problems come with an increase of computational costs due to an increase of global couplings. To compensate for that we consider a corresponding HDG method. For that, we need to introduce additional unknowns on the skeleton $\mathcal{F}_{h,S}$, the *facet unknowns*, which represent an approximation of the tangential trace of the solution in the Stokes region:

$$M_h := \left\{ \boldsymbol{v}_F \in \prod_{F \in \mathcal{F}_{h,S}} [\mathbb{P}^{k_f}(T)]^d, \quad \boldsymbol{v}_F \cdot \boldsymbol{n} = 0 \, \forall F \in \mathcal{F}_{h,S}, \quad \boldsymbol{v}_F = 0 \, \forall F \in \Gamma_{h,S}, \right\} \tag{3c}$$

where $k_f = \begin{cases} k & \text{if } k = 1 \\ k-1 & \text{if } k \geq 2 \end{cases}$. Functions in M_h are defined only on the mesh skeleton in the Stokes region $\mathcal{F}_{h,S}$ and have normal component *zero*, and vanish on the Stokes boundary Γ_S. Here, due to a technical difficulty in proving a norm equivalence result, see Lemma 1 below, we can not decrease the polynomial degree k_f to one order less for the lowest order case $k = 1$. Note however that in the numerical example below, we obtain optimal order results also for the choice $k_f = 0$ for $k = 1$. The reduction of k_f from k to $k-1$ results in an additional significant reduction of global couplings in arising linear systems for the Stokes part of the problem, cf. [24,25,29].

For the discretization of the velocity field we use the composite space

$$\underline{U}_h := \boldsymbol{\Sigma}_h \times M_h.$$

2.2.3 The Numerical Scheme

First, we introduce the L^2 projection Π for a fixed facet $F \in \mathcal{F}_{h,S}$:

$$\Pi : [\mathbb{P}^k(F)]^d \to [\mathbb{P}^{k_f}(F)]^d, \quad \int_F (\Pi f) v \, \mathrm{ds} = \int_F f \, v \, \mathrm{ds} \quad \forall v \in [\mathbb{P}^{k_f}(F)]^d.$$

Then, for all $\underline{\boldsymbol{u}}, \underline{\boldsymbol{v}} \in \underline{\boldsymbol{U}}_h$ and $q \in Q_h$, we introduce the bilinear and linear forms

$$
\begin{aligned}
a_{S,h}(\underline{\boldsymbol{u}}, \underline{\boldsymbol{v}}) := \sum_{T \in \mathcal{T}_{h,S}} \int_T 2\nu\, \varepsilon(\boldsymbol{u}_T) : \varepsilon(\boldsymbol{v}_T)\, \mathrm{dx} - \int_{\partial T} 2\nu\, \varepsilon(\boldsymbol{u}_T)\boldsymbol{n} \cdot [\![\underline{\boldsymbol{v}}^t]\!]\, \mathrm{ds} \\
- \int_{\partial T} 2\nu\, \varepsilon(\boldsymbol{v}_T)\boldsymbol{n} \cdot [\![\underline{\boldsymbol{u}}^t]\!]\, \mathrm{ds} + \int_{\partial T} \nu \frac{\alpha}{h} \Pi [\![\underline{\boldsymbol{u}}^t]\!] \cdot \Pi [\![\underline{\boldsymbol{v}}^t]\!]\, \mathrm{ds},
\end{aligned} \tag{4a}
$$

$$
a_D(\underline{\boldsymbol{u}}, \underline{\boldsymbol{v}}) := \sum_{T \in \mathcal{T}_{h,S}} \int_T K^{-1} \boldsymbol{u}_T \cdot \boldsymbol{v}_T\, \mathrm{dx}, \tag{4b}
$$

$$
a_I(\underline{\boldsymbol{u}}, \underline{\boldsymbol{v}}) := \sum_{F \in \mathcal{F}_{h,SD}} \int_F \gamma K^{-1/2} \boldsymbol{u}_F \cdot \boldsymbol{v}_F\, \mathrm{ds}, \tag{4c}
$$

$$
a_h(\underline{\boldsymbol{u}}, \underline{\boldsymbol{v}}) := a_{S,h}(\underline{\boldsymbol{u}}, \underline{\boldsymbol{v}}) + a_D(\underline{\boldsymbol{u}}, \underline{\boldsymbol{v}}) + a_I(\underline{\boldsymbol{u}}, \underline{\boldsymbol{v}}),
$$

$$
b(\underline{\boldsymbol{u}}, q) = - \sum_{T \in \mathcal{T}_h} \int_T \nabla \cdot \boldsymbol{u}_T q\, \mathrm{dx}, \tag{4d}
$$

$$
f_1(\underline{\boldsymbol{v}}) = \sum_{T \in \mathcal{T}_{h,S}} \int_T \boldsymbol{f}_S \cdot \boldsymbol{v}_T\, \mathrm{dx}, \tag{4e}
$$

$$
f_2(q) = \sum_{T \in \mathcal{T}_{h,D}} \int_T f_D\, q\, \mathrm{dx}, \tag{4f}
$$

where $[\![\underline{\boldsymbol{u}}^t]\!] = \boldsymbol{u}_T^t - \boldsymbol{u}_F$ is the (tangential) jump between interior and facet unknowns, and $\alpha = \alpha_0 k^2$ with α_0 a sufficiently large positive constant. We note that (only) as long as $\underline{\boldsymbol{u}}$, $\underline{\boldsymbol{v}}$ are finite element functions in $\underline{\boldsymbol{U}}_h$ we have

$$
\int_{\partial T} 2\nu\varepsilon(\boldsymbol{u}_T)\boldsymbol{n} \cdot [\![\underline{\boldsymbol{v}}^t]\!] ds = \int_{\partial T} 2\nu\varepsilon(\boldsymbol{u}_T)\boldsymbol{n} \cdot \Pi [\![\underline{\boldsymbol{v}}^t]\!] ds
$$

for (4a) as $2\nu\varepsilon(\boldsymbol{u}_T)\boldsymbol{n}$ is a polynomial of degree $k-1$ on each facet.

The numerical scheme then reads: Find $(\underline{\boldsymbol{u}}_h, p_h) \in \underline{\boldsymbol{U}}_h \times Q_h$ such that

$$
a_h(\underline{\boldsymbol{u}}_h, \underline{\boldsymbol{v}}_h) + b(\underline{\boldsymbol{v}}_h, p_h) = f_1(\underline{\boldsymbol{v}}_h), \quad \forall \underline{\boldsymbol{v}}_h \in \underline{\boldsymbol{U}}_h, \tag{5a}
$$

$$
b(\underline{\boldsymbol{u}}_h, q_h) = -f_2(q_h), \quad \forall q_h \in Q_h. \tag{5b}
$$

Remark 1 (Strong mass conservation) By the divergence conformity of the space $\boldsymbol{\Sigma}_h$, Eq. (5b) can be written as

$$
-\int_\Omega \nabla \cdot \boldsymbol{u}_{h,T}\, q_h\, \mathrm{dx} = -\int_\Omega \chi_D f_D\, q_h\, \mathrm{dx} \quad \forall q_h \in Q_h.
$$

Hence, $\nabla \cdot \boldsymbol{u}_{h,T} - \chi_D P_Q f_D \equiv 0$ where P_Q is the L^2-projection onto Q_h. This is a strong mass conservation in terms of $H(\mathrm{div}; \Omega)$.

We define the following seminorms:

$$|\underline{\boldsymbol{u}}|_{e,S}^2 := \sum_{T\in\mathcal{T}_{h,S}} \nu \left(\|\varepsilon(\boldsymbol{u}_T)\|_T^2 + \frac{1}{h}\|\Pi[\![\underline{\boldsymbol{u}}^t]\!]\|_{\partial T}^2 \right), \tag{6a}$$

$$|\underline{\boldsymbol{u}}|_{1,S}^2 := \sum_{T\in\mathcal{T}_{h,S}} \nu \left(\|\nabla \boldsymbol{u}_T\|_T^2 + \frac{1}{h}\|[\![\underline{\boldsymbol{u}}^t]\!]\|_{\partial T}^2 \right), \tag{6b}$$

$$|\underline{\boldsymbol{u}}|_{1*,S}^2 := \sum_{T\in\mathcal{T}_{h,S}} \nu \left(\|\nabla \boldsymbol{u}_T\|_T^2 + h^2\|\nabla^2(\boldsymbol{u}_T)\|_T^2 + \frac{1}{h}\|\Pi[\![\underline{\boldsymbol{u}}^t]\!]\|_{\partial T}^2 \right), \tag{6c}$$

$$|\underline{\boldsymbol{u}}|_D^2 := \sum_{T\in\mathcal{T}_{h,D}} \|K^{-1/2}\boldsymbol{u}_T\|_T^2, \tag{6d}$$

$$|\underline{\boldsymbol{u}}|_I^2 := \sum_{F\in\mathcal{F}_{h,SD}} \|\gamma^{1/2}K^{-1/4}\boldsymbol{u}_F\|_F^2, \tag{6e}$$

where $\|\cdot\|_D$ denotes the standard L^2-norm on the domain D. We note that the semi-norms in (6a)–(6c) are slight variations of each other with different handling of the volume control ($\varepsilon(\boldsymbol{u}_T)$ vs. $\nabla(\boldsymbol{u}_T)$), the jump terms ($\Pi[\![\underline{\boldsymbol{u}}^t]\!]$ vs. $[\![\underline{\boldsymbol{u}}^t]\!]$) and control in higher order derivatives ($\nabla^2(\boldsymbol{u}_T)$ vs. no control). All three norms (and their equivalence on discrete spaces) will be used in the analysis below.

Throughout this work, we write

$$A \preceq B$$

to indicate that there exists a constant C, independent of the mesh size h and the numerical solution, such that $A \le CB$.

2.2.4 Wellposedness

Lemma 1 *For $\underline{\boldsymbol{v}}_h \in \underline{\boldsymbol{U}}_h$, there holds*

$$|\underline{\boldsymbol{v}}_h|_{1*,S} \preceq |\underline{\boldsymbol{v}}_h|_{1,S}, \quad \textit{and} \quad |\underline{\boldsymbol{v}}_h|_{1,S} \preceq |\underline{\boldsymbol{v}}_h|_{e,S}.$$

Proof Take $\underline{\boldsymbol{v}}_h = (\boldsymbol{v}_T, \boldsymbol{v}_F) \in \underline{\boldsymbol{U}}_h$. The first inequality comes from the inverse inequality for finite dimensional spaces and stability of the L^2 projection. To prove the second inequality, we shall use the following discrete Korn's inequality [6]:

$$|\underline{\boldsymbol{v}}_h|_{1,S}^2 \preceq \sum_{T\in\mathcal{T}_{h,S}} \nu \left(\|\varepsilon(\boldsymbol{v}_T)\|_T^2 + \frac{1}{h}\|[\![\underline{\boldsymbol{v}}_h^t]\!]\|_{\partial T}^2 \right).$$

Since the space of rigid motions $RM(T)$ lies in $[\mathbb{P}_1(T)]^d \subset [\mathbb{P}_{k_f}(T)]^d$,

$$\begin{aligned}
h^{-1/2}\|[\![\underline{\boldsymbol{v}}_h^t]\!]\|_{\partial T} &= h^{-1/2}\|\Pi[\![\underline{\boldsymbol{v}}_h^t]\!]\|_{\partial T} + h^{-1/2}\|\boldsymbol{v}_T - \Pi\, \boldsymbol{v}_T\|_{\partial T} \\
&= h^{-1/2}\|\Pi[\![\underline{\boldsymbol{v}}_h^t]\!]\|_{\partial T} + h^{-1/2} \inf_{\Lambda\in RM(T)} \|(\boldsymbol{v}_T - \Lambda) - \Pi\,(\boldsymbol{v}_T - \Lambda)\|_{\partial T} \\
&\le h^{-1/2}\|\Pi[\![\underline{\boldsymbol{v}}_h^t]\!]\|_{\partial T} + h^{-1/2} \inf_{\Lambda\in RM(T)} \|(\boldsymbol{v}_T - \Lambda) - \overline{(\boldsymbol{v}_T - \Lambda)}\|_{\partial T} \\
&\le h^{-1/2}\|\Pi[\![\underline{\boldsymbol{v}}_h^t]\!]\|_{\partial T} + C \inf_{\Lambda\in RM(T)} \|\nabla(\boldsymbol{v}_T - \Lambda)\|_T \\
&\le h^{-1/2}\|\Pi[\![\underline{\boldsymbol{v}}_h^t]\!]\|_{\partial T} + C\|\varepsilon(\boldsymbol{v}_T)\|_T,
\end{aligned}$$

where $\overline{\star}$ is the average of $\star$ in T, and the last step follows from the local Korn's inequality [30, Lemma 4.1]. The proof is completed by combing the above two inequalities. □

Lemma 2 *The bilinear form $a_{S,h}(\cdot,\cdot)$ chosen in the Stokes subdomain Ω_S has the following properties:*

(a) ***Coercivity:*** *For α_0 sufficiently large, there holds*

$$|\underline{\boldsymbol{v}}_h|_{1,S}^2 \preceq a_{S,h}(\underline{\boldsymbol{v}}_h, \underline{\boldsymbol{v}}_h) \quad \forall \underline{\boldsymbol{v}}_h \in \underline{\boldsymbol{U}}_h. \tag{7a}$$

(b) ***Boundedness:*** *There holds*

$$a_{S,h}(\underline{\boldsymbol{v}}, \underline{\boldsymbol{w}}) \preceq |\underline{\boldsymbol{v}}|_{1*,S} |\underline{\boldsymbol{w}}|_{1*,S}, \quad \forall \underline{\boldsymbol{v}}, \underline{\boldsymbol{w}} \in \underline{\boldsymbol{V}} + \underline{\boldsymbol{U}}_h, \tag{7b}$$

where

$$\begin{aligned}\underline{\boldsymbol{V}} = \Big\{ \left(\boldsymbol{v}_T, (\boldsymbol{v}_T)^t|_{\mathcal{F}_{h,S}}\right) : \boldsymbol{v}_T|_{\Omega_S} \in \boldsymbol{H}^2(\Omega_S), \quad \boldsymbol{v}_T|_{\Gamma_S} = 0, \\ \boldsymbol{v}_T|_{\Omega_D} \in \boldsymbol{H}^1(\Omega_D), \quad \boldsymbol{v}_T \cdot \boldsymbol{n}|_{\Gamma_D} = 0 \Big\}.\end{aligned} \tag{7c}$$

(c) ***Consistency:*** *Let $(\boldsymbol{u}_S, p_S) \in \boldsymbol{H}^2(\Omega_S) \times H^1(\Omega_S)$ be part of the solution to Eqs. (1) and (2), and set $\underline{\boldsymbol{u}} = (\boldsymbol{u}_S, \boldsymbol{u}_S^t|_{\mathcal{F}_{h,S}})$. Then, for all $\boldsymbol{v} = (\boldsymbol{v}_T, \boldsymbol{v}_F) \in \underline{\boldsymbol{V}} + \underline{\boldsymbol{U}}_h$, there holds*

$$\begin{aligned} a_{S,h}(\underline{\boldsymbol{u}}, \boldsymbol{v}) = &\int_{\Omega_S} (\boldsymbol{f}_S - \nabla p_S) \cdot \boldsymbol{v}_T \,\mathrm{dx} + \int_{\Gamma_{SD}} (2\nu\varepsilon(\boldsymbol{u}_S)\boldsymbol{n}\cdot\boldsymbol{n})\boldsymbol{v}_T \cdot \boldsymbol{n} \,\mathrm{ds} \\ &- \int_{\Gamma_{SD}} \gamma K^{-1/2} \boldsymbol{u}_S^t \cdot \boldsymbol{v}_F \,\mathrm{ds}. \end{aligned} \tag{7d}$$

Proof Take $\underline{\boldsymbol{v}}_h = (\boldsymbol{v}_T, \boldsymbol{v}_F) \in \underline{\boldsymbol{U}}_h$. By Lemma 1, we only need to prove coercivity on the weaker seminorm $|\cdot|_{e,S}$. Since $\varepsilon(\boldsymbol{v}_T)\boldsymbol{n}|_F \in [\mathbb{P}^{k-1}(F)]^d$, we have

$$\begin{aligned} \int_{\partial T} \nu\, \varepsilon(\boldsymbol{v}_T)\boldsymbol{n} \cdot [\![\underline{\boldsymbol{v}}_h^t]\!] \,\mathrm{ds} &= \int_{\partial T} \nu\, \varepsilon(\boldsymbol{v}_T)\boldsymbol{n} \cdot \Pi[\![\underline{\boldsymbol{v}}_h^t]\!] \,\mathrm{ds} \\ &\le \nu \|\varepsilon(\boldsymbol{v}_T)\boldsymbol{n}\|_{\partial T} \|\Pi[\![\underline{\boldsymbol{v}}_h^t]\!]\|_{\partial T} \le C\,\nu h_T^{-1/2} \|\varepsilon(\boldsymbol{v}_T)\|_T \|\Pi[\![\underline{\boldsymbol{v}}_h^t]\!]\|_{\partial T} \\ &\le \frac{1}{4}\nu\|\varepsilon(\boldsymbol{v}_T)\|_T^2 + C^2\,\nu h_T^{-1} \|\Pi[\![\underline{\boldsymbol{v}}_h^t]\!]\|_{\partial T}^2, \end{aligned}$$

where C is the constant arising in the trace-inverse inequality [38]. Now,

$$\begin{aligned} a_{S,h}(\underline{\boldsymbol{v}}_h, \underline{\boldsymbol{v}}_h) = &\sum_{T\in\mathcal{T}_{h,S}} \int_T 2\nu\,\varepsilon(\boldsymbol{v}_T) : \varepsilon(\boldsymbol{v}_T)\,\mathrm{dx} - 4\int_{\partial T} \nu\,\varepsilon(\boldsymbol{v}_T)\boldsymbol{n}\cdot[\![\underline{\boldsymbol{v}}_h^t]\!]\,\mathrm{ds} \\ &+ \int_{\partial T} \nu\frac{\alpha}{h}\Pi[\![\underline{\boldsymbol{v}}_h^t]\!]\cdot\Pi[\![\underline{\boldsymbol{v}}_h^t]\!]\,\mathrm{ds} \\ \ge &\sum_{T\in\mathcal{T}_{h,S}} \nu\left(\|\varepsilon(\boldsymbol{v}_T)\|_T^2 + \left(\frac{\alpha}{h} - 4C^2h_T^{-1}\right)\|\Pi[\![\underline{\boldsymbol{v}}_h^t]\!]\|_{\partial T}^2\right). \end{aligned}$$

The right hand side of the above expression is an upper bound for $|\underline{\boldsymbol{v}}_h|_{1,S}^2$ for sufficiently large α_0. This completes the proof of coercivity (7a).

Boundedness (7b) is a direct consequence of the Cauchy–Schwarz inequality and the trace inequality.

Finally, let us prove the consistency result (7d). By definition, we have

$$
\begin{aligned}
a_{S,h}(\underline{\boldsymbol{u}}, \boldsymbol{v}) &= \sum_{T\in\mathcal{T}_{h,S}} \int_T 2\nu\, \varepsilon(\boldsymbol{u}_S) : \varepsilon(\boldsymbol{v}_T)\,\mathrm{dx} - \int_{\partial T} 2\nu\, \varepsilon(\boldsymbol{u}_S)\boldsymbol{n}\cdot [\![\underline{\boldsymbol{v}}^t]\!]\,\mathrm{ds}\\
&= \sum_{T\in\mathcal{T}_{h,S}} \int_T 2\nu\, \varepsilon(\boldsymbol{u}_S) : \varepsilon(\boldsymbol{v}_T)\,\mathrm{dx} - \int_{\partial T} 2\nu\, \varepsilon(\boldsymbol{u}_S)\boldsymbol{n}\cdot \left(\boldsymbol{v}_T^t - \boldsymbol{v}_F\right)\,\mathrm{ds}\\
&= \sum_{T\in\mathcal{T}_{h,S}} \int_T -(\nabla\cdot 2\nu\, \varepsilon(\boldsymbol{u}_S))\cdot \boldsymbol{v}_T\,\mathrm{dx} + \int_{\partial T} 2\nu\, \varepsilon(\boldsymbol{u}_S)\boldsymbol{n}\cdot \left(\boldsymbol{v}_T - \boldsymbol{v}_T^t\right)\,\mathrm{ds}\\
&\quad + \int_{\partial T} 2\nu\, \varepsilon(\boldsymbol{u}_S)\boldsymbol{n}\cdot \boldsymbol{v}_F\,\mathrm{ds}.
\end{aligned}
\tag{8}
$$

By Eq. (1a), we have

$$
\sum_{T\in\mathcal{T}_{h,S}} \int_T -(\nabla\cdot 2\nu\, \varepsilon(\boldsymbol{u}_S))\cdot \boldsymbol{v}_T\,\mathrm{dx} = \int_{\Omega_S} (\boldsymbol{f}_S - \nabla p_S)\cdot \boldsymbol{v}_T\,\mathrm{dx}.
$$

By smoothness of $\boldsymbol{u}$, $H(\mathrm{div})$-conformity of $\boldsymbol{v}_T$, and the boundary conditions (2c)–(2d), the first boundary term on the right hand side of (8) can be simplified as

$$
\sum_{T\in\mathcal{T}_{h,S}} \int_{\partial T} 2\nu\, \varepsilon(\boldsymbol{u}_S)\boldsymbol{n}\cdot \left(\boldsymbol{v}_T - \boldsymbol{v}_T^t\right)\,\mathrm{ds} = \int_{\Gamma_{SD}} 2\nu\, \varepsilon(\boldsymbol{u}_S)\boldsymbol{n}\cdot \boldsymbol{n}(\boldsymbol{v}_T\cdot\boldsymbol{n})\,\mathrm{ds},
$$

and the second boundary term can be simplified as

$$
\begin{aligned}
\sum_{T\in\mathcal{T}_{h,S}} \int_{\partial T} 2\nu\, \varepsilon(\boldsymbol{u}_S)\boldsymbol{n}\cdot \boldsymbol{v}_F\,\mathrm{ds} &= \int_{\Gamma_{SD}} 2\nu\, (\varepsilon(\boldsymbol{u}_S)\boldsymbol{n})^t\cdot \boldsymbol{v}_F\,\mathrm{ds}\\
&= -\int_{\Gamma_{SD}} \gamma K^{-1/2}\boldsymbol{u}_S^t\cdot \boldsymbol{v}_F\,\mathrm{ds}.
\end{aligned}
$$

The equality (7d) is obtained by combining the above identities. □

Proposition 1 *For α_0 sufficiently large, there exists a unique solution $(\underline{\boldsymbol{u}}_h, p_h) \in \underline{\boldsymbol{U}}_h \times Q_h$ for the scheme* (5).

Proof Since the equations in (5) form a quadratic system, we only need to proof uniqueness of the solution, that is, the only solution to the scheme (5) with *vanishing* right hand sides is *zero*.

Assuming $f_1 = f_2 = 0$, taking $\underline{\boldsymbol{v}}_h = \underline{\boldsymbol{u}}_h$ and $q_h = -p_h$ in (5), and adding up the resulting equations, we obtain

$$
a_h(\underline{\boldsymbol{u}}_h, \underline{\boldsymbol{u}}_h) = a_{S,h}(\underline{\boldsymbol{u}}_h, \underline{\boldsymbol{u}}_h) + |\underline{\boldsymbol{u}}_h|_D^2 + |\underline{\boldsymbol{u}}_h|_I^2 = 0.
$$

Hence, for sufficiently large α_0, $\underline{\boldsymbol{u}}_h = 0$ by (7a) in Lemma 2. Then, Eq. (5a) implies that $b(\underline{\boldsymbol{v}}_h, p_h) = -\int_\Omega \nabla\cdot\boldsymbol{v}_T\, p_h\,\mathrm{dx} = 0$. Due to the special compatibility of pressure and velocity spaces we can take $\boldsymbol{v}_T$ be such that $\nabla\cdot\boldsymbol{v}_T = p_h$ which yields $p_h = 0$ and completes the proof. □

3 Error Analysis

In this section, we present our main result on the velocity error estimates. The analysis is based on the results in [20,25].

Denote P_M, P_Q as the standard L^2 projections onto the spaces M_h and Q_h, and Π_V as the following $H(\mathrm{div})$-conforming BDM projection [5]: for all $T \in \mathcal{T}_h$,

$$\int_T \Pi_V \boldsymbol{u} \cdot \boldsymbol{v}\,\mathrm{d}x = \int_T \boldsymbol{u} \cdot \boldsymbol{v}\,\mathrm{d}x, \qquad \forall \boldsymbol{v} \in \nabla\mathbb{P}^{k-1}(T) \oplus B^k(T),$$
$$\int_F \Pi_V \boldsymbol{u} \cdot \boldsymbol{n}\mu\,\mathrm{d}s = \int_F \boldsymbol{u} \cdot \boldsymbol{n}\mu\,\mathrm{d}s, \qquad \forall \boldsymbol{v} \in \mathbb{P}^k(F), \forall F \in \mathcal{F}(T),$$

where $B^k(T) := \{\boldsymbol{v} \in [\mathbb{P}^k(T)]^d : \nabla\cdot\boldsymbol{v}|_T = 0, \quad \boldsymbol{v}\cdot\boldsymbol{n}|_{\partial T} = 0\}$ is the divergence-free bubble space.

The following commuting diagram property of the projection pair (Π_V, P_Q) is well-known:

$$\nabla\cdot\Pi_V\boldsymbol{\phi} = P_Q\nabla\cdot\boldsymbol{\phi}, \quad \forall\boldsymbol{\phi} \in \boldsymbol{H}^1(\Omega).$$

We define discrete error $(\underline{\boldsymbol{e}}_u, e_p)$ and an approximation error $(\underline{\boldsymbol{\delta}}_u, \delta_p)$ to simplify notation:

$$\boldsymbol{e}_{u,T} = \Pi_V\boldsymbol{u} - \boldsymbol{u}_{h,T}, \quad \boldsymbol{e}_{u,F} = P_M\boldsymbol{u}^t - \boldsymbol{u}_{h,F}, \qquad \underline{\boldsymbol{e}}_u = (\boldsymbol{e}_{u,T}, \boldsymbol{e}_{u,F}), \tag{9a}$$
$$\boldsymbol{\delta}_{u,T} = \Pi_V\boldsymbol{u} - \boldsymbol{u}, \quad \boldsymbol{\delta}_{u,F} = P_M\boldsymbol{u}^t|_{\mathcal{F}_{h,S}} - \boldsymbol{u}^t|_{\mathcal{F}_{h,S}}, \qquad \underline{\boldsymbol{\delta}}_u = (\boldsymbol{\delta}_{u,T}, \boldsymbol{\delta}_{u,F}), \tag{9b}$$
$$e_p = P_Q p - p_h, \quad \delta_p = P_Q p - p. \tag{9c}$$

Here $\boldsymbol{u}^t|_{\mathcal{F}_{h,S}}$ is the restriction of the tangential component of $\boldsymbol{u}$ on the facets $\mathcal{F}_{h,S}$.

3.1 Energy Norm Estimate

Theorem 1 *Assume that the solution $(\boldsymbol{u}, p)$ of the Eqs. (1), (2) is in $\boldsymbol{X}_s \times Y_s$ where*

$$\boldsymbol{X}_s = \{\boldsymbol{v} \in H_0(\mathrm{div};\Omega) : \quad \boldsymbol{v}|_{\Omega_S} \in \boldsymbol{H}^s(\Omega_S),\ \boldsymbol{v}|_{\Omega_D} \in \boldsymbol{H}^{s-1}(\Omega_D), \boldsymbol{v}|_{\Gamma_S} = 0\},$$
$$Y_s = \{q \in L_0^2(\Omega) : \quad q|_{\Omega_S} \in H^{s-1}(\Omega_S),\ q|_{\Omega_D} \in H^s(\Omega_D)\}.$$

for some $s \in [2, k+1]$. Then, for stabilization parameter α_0 sufficiently large, the solution $\underline{\boldsymbol{u}}_h$ to the system (5) has the energy error estimate

$$|\underline{\boldsymbol{e}}_u|_{1,S} + |\underline{\boldsymbol{e}}_u|_I + |\underline{\boldsymbol{e}}_u|_D \preceq |\underline{\boldsymbol{\delta}}_u|_{1*,S} + |\underline{\boldsymbol{\delta}}_u|_D \tag{10a}$$
$$\preceq h^{s-1}\left(\nu\|\boldsymbol{u}\|_{\boldsymbol{H}^s(\Omega_S)} + \lambda_{\min}^{-1/2}\|\boldsymbol{u}\|_{\boldsymbol{H}^{s-1}(\Omega_D)}\right), \tag{10b}$$

where $\lambda_{\min}$ is the minimal eigenvalue of the permeability tensor K.

The following Lemmas will be used to prove Theorem 1.

Lemma 3 (Approximation) *For $\boldsymbol{u} \in \boldsymbol{H}^s(\Omega_S)$ with some $s \in [2, k+1]$, there holds*

$$|\underline{\boldsymbol{\delta}}_u|_{1*,S} \preceq \nu^{1/2}h^{s-1}\|\boldsymbol{u}\|_{\boldsymbol{H}^s(\Omega_S)}.$$

Proof We have

$$|\underline{\boldsymbol{\delta}}_u|_{1*,S}^2 = \sum_{T\in\mathcal{T}_{h,S}} \nu\left(\|\nabla\boldsymbol{\delta}_{u,T}\|_T^2 + h^2\|\nabla^2(\boldsymbol{\delta}_{u,T})\|_T^2 + \frac{1}{h}\|\Pi[\![\underline{\boldsymbol{\delta}}_u^t]\!]\|_{\partial T}^2\right),$$

where we obtain the desired bounds for the first two terms by standard estimates for the BDM projection. For the latter boundary term, we have

$$\begin{aligned}\|\Pi[\![\underline{\boldsymbol{\delta}}_u^t]\!]\|_{\partial T}^2 &= \|P_M[\![\underline{\boldsymbol{\delta}}_u^t]\!]\|_{\partial T}^2 = \|P_M\left((\Pi_V \boldsymbol{u})^t - P_M \boldsymbol{u}^t\right)\|_{\partial T}^2 \\ &= \|P_M\left((\Pi_V \boldsymbol{u})^t - \boldsymbol{u}^t\right)\|_{\partial T}^2 \leq \|\Pi_V \boldsymbol{u} - \boldsymbol{u}\|_{\partial T}^2,\end{aligned}$$

The above right hand side is further handled by a trace inequality:

$$\|\Pi_V \boldsymbol{u} - \boldsymbol{u}\|_{\partial T} \preceq h^{-\frac{1}{2}}\|\Pi_V \boldsymbol{u} - \boldsymbol{u}\|_T + h^{\frac{1}{2}}\|\nabla(\Pi_V \boldsymbol{u} - \boldsymbol{u})\|_T \preceq h^{s-\frac{1}{2}}\|\boldsymbol{u}\|_{\boldsymbol{H}^s(T)}.$$

□

Lemma 4 (Galerkin orthogonality) *Let the assumptions of Theorem 1 hold. Denoting* $\underline{\boldsymbol{u}} = (\boldsymbol{u}, \boldsymbol{u}^t|_{\mathcal{F}_{h,S}})$*, then*

$$a_h(\underline{\boldsymbol{u}} - \underline{\boldsymbol{u}}_h, \underline{\boldsymbol{v}}_h) + b(\underline{\boldsymbol{v}}_h, p - p_h) = 0, \quad \forall \underline{\boldsymbol{v}}_h \in \underline{\boldsymbol{U}}_h, \tag{11a}$$

$$b(\underline{\boldsymbol{u}} - \underline{\boldsymbol{u}}_h, q_h) = 0, \quad \forall q_h \in Q_h. \tag{11b}$$

Proof Let $\boldsymbol{v} = (\boldsymbol{v}_T, \boldsymbol{v}_F) \in \underline{\boldsymbol{V}} + \underline{\boldsymbol{U}}_h$, where the space $\underline{\boldsymbol{V}}$ is given by (7c). By smoothness of p and boundary conditions (2d), (2e), we have

$$\begin{aligned}b(\boldsymbol{v}, p) &= -\int_\Omega \nabla\cdot\boldsymbol{v}_T\, p\, \mathrm{dx} \\ &= \int_{\Omega_D} \boldsymbol{v}_T \cdot \nabla p_D\, \mathrm{dx} + \int_{\Omega_S} \boldsymbol{v}_T \cdot \nabla p_S\, \mathrm{dx} - \int_{\Gamma_{SD}} \boldsymbol{v}_T \cdot \boldsymbol{n}(p_S - p_D)\, \mathrm{ds},\end{aligned}$$

where the normal direction on Γ_{SD} points outward of Ω_S. Hence, by (7d) and boundary condition (2b), we get

$$\begin{aligned}a_h(\underline{\boldsymbol{u}}, \boldsymbol{v}) + b(\boldsymbol{v}, p) &= \int_{\Omega_S} \boldsymbol{f}_S \cdot \boldsymbol{v}_T\, \mathrm{dx} + \int_{\Omega_D} (K^{-1}\boldsymbol{u}_D + \nabla p_D)\cdot \boldsymbol{v}_T\, \mathrm{dx} \\ &\quad - \int_{\Gamma_{SD}} (p_S - p_D - 2\nu\varepsilon(\boldsymbol{u}_S)\boldsymbol{n}\cdot\boldsymbol{n})\boldsymbol{v}_T \cdot \boldsymbol{n}\, \mathrm{ds} \\ &= \int_{\Omega_S} \boldsymbol{f}_S \boldsymbol{v}_T\, \mathrm{dx}.\end{aligned} \tag{12}$$

Moreover, for any $q_h \in Q_h$, we have

$$b(\underline{\boldsymbol{u}}, q_h) = -\int_\Omega \nabla\cdot\boldsymbol{u}\, q_h\, \mathrm{dx} = -\int_{\Omega_D} f_D\, q_h\, \mathrm{dx}.$$

We complete the proof by comparing the above equations with the scheme (5). □

Now, we are ready to prove Theorem 1.

Proof of Theorem 1

By definition of the projections P_Q and Π_V, we have

$$b(\underline{\boldsymbol{v}}_h, \delta_p) = 0 \quad \forall \underline{\boldsymbol{v}}_h \in \underline{\boldsymbol{U}}_h, \text{ and } b(\underline{\boldsymbol{\delta}}_u, q_h) = 0 \quad \forall q_h \in Q_h.$$

Hence, by Lemma 4, the following error equation holds

$$\begin{aligned}a_h(\underline{\boldsymbol{e}}_u, \underline{\boldsymbol{v}}_h) + b(\underline{\boldsymbol{v}}_h, e_p) &= -a_h(\underline{\boldsymbol{\delta}}_u, \underline{\boldsymbol{v}}_h), \quad \forall \underline{\boldsymbol{v}}_h \in \underline{\boldsymbol{U}}_h, \\ b(\underline{\boldsymbol{e}}_u, q_h) &= 0, \quad \forall q_h \in Q_h.\end{aligned}$$

Taking $\underline{\boldsymbol{v}}_h = \underline{\boldsymbol{e}}_u$ in the first equation and $q_h = -e_p$ in the second equation, and adding, we obtain

$$a_h(\underline{\boldsymbol{e}}_u, \underline{\boldsymbol{e}}_u) = -a_h(\underline{\boldsymbol{\delta}}_u, \underline{\boldsymbol{e}}_u) = -a_{S,h}(\underline{\boldsymbol{\delta}}_u, \underline{\boldsymbol{e}}_u) - a_D(\underline{\boldsymbol{\delta}}_u, \underline{\boldsymbol{e}}_u) - \underbrace{a_I(\underline{\boldsymbol{\delta}}_u, \underline{\boldsymbol{e}}_u)}_{=0}. \tag{13}$$

where the last part vanishes due to the definition of the L^2 projection P_M,

$$a_I(\underline{\boldsymbol{\delta}}_u, \underline{\boldsymbol{e}}_u) = 0.$$

Now, with continuity, cf. Lemma 2 and the norm equivalence on $\underline{\boldsymbol{U}}_h$ of Lemma 1 we have

$$a_{S,h}(\underline{\boldsymbol{\delta}}_u, \underline{\boldsymbol{e}}_u) \preceq |\underline{\boldsymbol{\delta}}_u|_{1*,S} |\underline{\boldsymbol{e}}_u|_{1*,S} \preceq |\underline{\boldsymbol{\delta}}_u|_{1*,S} |\underline{\boldsymbol{e}}_u|_{1,S}$$

which combined with coercivity from Lemma 2 yields

$$\begin{aligned} |\underline{\boldsymbol{e}}_u|_{1,S}^2 + |\underline{\boldsymbol{e}}_u|_I^2 + |\underline{\boldsymbol{e}}_u|_D^2 &\preceq a_h(\underline{\boldsymbol{e}}_u, \underline{\boldsymbol{e}}_u) = -a_{S,h}(\underline{\boldsymbol{\delta}}_u, \underline{\boldsymbol{e}}_u) - a_D(\underline{\boldsymbol{\delta}}_u, \underline{\boldsymbol{e}}_u) \\ &\preceq \left(|\underline{\boldsymbol{\delta}}_u|_{1*,S}^2 + |\underline{\boldsymbol{\delta}}_u|_D^2 \right)^{\frac{1}{2}} \left(|\underline{\boldsymbol{e}}_u|_{1,S}^2 + |\underline{\boldsymbol{e}}_u|_D^2 \right)^{\frac{1}{2}} \end{aligned}$$

which implies (10a). We bound both terms on the right hand side of (10a) to obtain (10b). There holds

$$|\underline{\boldsymbol{\delta}}_u|_D = \|K^{-1/2} \boldsymbol{\delta}_{u,T}\|_{\Omega_D}\| \preceq \lambda_{\min}^{-1/2} h^{s-1} \|\boldsymbol{u}\|_{\boldsymbol{H}^{s-1}(\Omega_D)}.$$

and by Lemma 3, we further have

$$|\underline{\boldsymbol{\delta}}_u|_{1*,S} \preceq (\nu^{1/2} h^{s-1} \|\boldsymbol{u}\|_{\boldsymbol{H}^s(\Omega_S)}).$$

This completes the proof. □

3.2 L^2-Estimate in the Stokes Subdomain

We will use the following dual problem: Assume $(\boldsymbol{u}^*, p^*)$ solve Eqs. (1), (2) with source terms $\boldsymbol{f}_S = \boldsymbol{\psi}$ and $f_D = 0$, and further assume the following regularity estimates:

$$\|\boldsymbol{u}^*\|_{\boldsymbol{H}^{1+r}(\Omega_S)} \le C\|\boldsymbol{\psi}\|_{\Omega_S}, \qquad \|\boldsymbol{u}^*\|_{\boldsymbol{H}^{r}(\Omega_D)} \le C\|\boldsymbol{\psi}\|_{\Omega_S}, \tag{14a}$$

$$\|p^*\|_{\boldsymbol{H}^{r}(\Omega_S)} \le C\|\boldsymbol{\psi}\|_{\Omega_S}, \qquad \|p^*\|_{\boldsymbol{H}^{1+r}(\Omega_D)} \le C\|\boldsymbol{\psi}\|_{\Omega_S}, \tag{14b}$$

for some real number $1/2 < r \le 1$. This assumption is justified, for instance if Ω_S and Ω_D are convex.

Theorem 2 *Let the assumptions of Theorem 1 hold. Assume further the regularity estimates* (14) *hold. Then, the following error estimate holds*

$$\|\boldsymbol{u} - \boldsymbol{u}_{h,T}\|_{\Omega_S} \preceq h^{s-1+r} (\|\boldsymbol{u}\|_{\boldsymbol{H}^s(\Omega_S)} + \|\boldsymbol{u}\|_{\boldsymbol{H}^{s-1}(\Omega_D)} + \|f_D\|_{H^{s-1}(\Omega_D)}). \tag{15}$$

Proof Let $(\boldsymbol{u}^*, p^*)$ be solutions to (1), (2) with $\boldsymbol{f}_S = \boldsymbol{u} - \boldsymbol{u}_{h,T}$, and $f_D = 0$. Denote $\underline{\boldsymbol{u}}^* = (\boldsymbol{u}^*, (\boldsymbol{u}^*)^t|_{\mathcal{F}_{h,S}})$. By (12), we get

$$a_h(\underline{\boldsymbol{u}}^*, \underline{\boldsymbol{v}}) + b(\underline{\boldsymbol{v}}, p^*) = (\boldsymbol{u} - \boldsymbol{u}_{h,T}, \boldsymbol{v}_T)_{\Omega_S}, \quad \forall \boldsymbol{v} \in \underline{\boldsymbol{V}} + \underline{\boldsymbol{U}}_h.$$

Taking $\underline{\boldsymbol{v}} = \underline{\boldsymbol{u}} - \underline{\boldsymbol{u}}_h$, we get

$$\begin{aligned} \|\boldsymbol{u} - \boldsymbol{u}_{h,T}\|_{\Omega_S}^2 &= a_h(\underline{\boldsymbol{u}}^*, \underline{\boldsymbol{u}} - \underline{\boldsymbol{u}}_h) + b(\underline{\boldsymbol{u}} - \underline{\boldsymbol{u}}_h, p^*) \\ &= a_h(\underline{\boldsymbol{u}} - \underline{\boldsymbol{u}}_h, \underline{\boldsymbol{u}}^*) + b(\underline{\boldsymbol{u}} - \underline{\boldsymbol{u}}_h, p^*) \end{aligned}$$

Let us bound each of the above terms on the right hand side. We denote $\underline{\boldsymbol{u}}_h^* = (\Pi_V \boldsymbol{u}^*, P_M(\boldsymbol{u}^*)^t)$. We have $\nabla\cdot\Pi_V \boldsymbol{u}^* = \nabla\cdot\boldsymbol{u}^* = 0$. Taking $\underline{\boldsymbol{v}}_h = \underline{\boldsymbol{u}}_h^*$ in (11a), we get $a_h(\underline{\boldsymbol{u}} - \underline{\boldsymbol{u}}_h, \underline{\boldsymbol{u}}_h^*) = 0$. Hence,

$$a_h(\underline{\boldsymbol{u}} - \underline{\boldsymbol{u}}_h, \underline{\boldsymbol{u}}^*) = a_h(\underline{\boldsymbol{u}} - \underline{\boldsymbol{u}}_h, \underline{\boldsymbol{u}}^* - \underline{\boldsymbol{u}}_h^*).$$

We have

$$\begin{aligned}
a_{S,h}(\underline{\boldsymbol{u}} - \underline{\boldsymbol{u}}_h, \underline{\boldsymbol{u}}^* - \underline{\boldsymbol{u}}_h^*) &\preceq |\underline{\boldsymbol{u}} - \underline{\boldsymbol{u}}_h|_{1*,S} |\underline{\boldsymbol{u}}^* - \underline{\boldsymbol{u}}_h^*|_{1*,S} \\
&\preceq \nu^{1/2} h^r |\boldsymbol{u}^*|_{\boldsymbol{H}^{1+r}(\Omega_S)} |\underline{\boldsymbol{u}} - \underline{\boldsymbol{u}}_h|_{1*,S}, \\
a_I(\underline{\boldsymbol{u}} - \underline{\boldsymbol{u}}_h, \underline{\boldsymbol{u}}^* - \underline{\boldsymbol{u}}_h^*) &\leq |\underline{\boldsymbol{u}} - \underline{\boldsymbol{u}}_h|_I |\underline{\boldsymbol{u}}^* - \underline{\boldsymbol{u}}_h^*|_I \\
&\preceq \gamma^{1/2} \lambda_{\min}^{-1/4} h^{1/2+r} |\boldsymbol{u}^*|_{\boldsymbol{H}^{1+r}(\Omega_S)} |\underline{\boldsymbol{u}} - \underline{\boldsymbol{u}}_h|_I, \\
a_D(\underline{\boldsymbol{u}} - \underline{\boldsymbol{u}}_h, \underline{\boldsymbol{u}}^* - \underline{\boldsymbol{u}}_h^*) &\leq |\underline{\boldsymbol{u}} - \underline{\boldsymbol{u}}_h|_D |\underline{\boldsymbol{u}}^* - \underline{\boldsymbol{u}}_h^*|_D \\
&\preceq \lambda_{\min}^{-1/2} h^r |\boldsymbol{u}^*|_{\boldsymbol{H}^r(\Omega_D)} |\underline{\boldsymbol{u}} - \underline{\boldsymbol{u}}_h|_D.
\end{aligned}$$

Combing the above estimates with the regularity assumption (14), we get

$$a_h(\underline{\boldsymbol{u}} - \underline{\boldsymbol{u}}_h, \underline{\boldsymbol{u}}^*) \preceq h^r \left(|\underline{\boldsymbol{u}} - \underline{\boldsymbol{u}}_h|_{1*,S} + h^{1/2} |\underline{\boldsymbol{u}} - \underline{\boldsymbol{u}}_h|_I + |\underline{\boldsymbol{u}} - \underline{\boldsymbol{u}}_h|_D \right) \|\boldsymbol{u} - \boldsymbol{u}_{h,T}\|_{\Omega_S}.$$

The norm in the parentheses of the above right hand side is bounded by $Ch^{s-1}(\|\boldsymbol{u}\|_{\boldsymbol{H}^s(\Omega_S)} + \|\boldsymbol{u}\|_{\boldsymbol{H}^{s-1}(\Omega_D)})$ by Theorem 1.

On the other hand, we have

$$\begin{aligned}
b(\underline{\boldsymbol{u}} - \underline{\boldsymbol{u}}_h, p^*) = &- \int_\Omega \nabla\cdot(\boldsymbol{u} - \underline{\boldsymbol{u}}_h) p^* \,\mathrm{dx} \\
= &- \int_{\Omega_D} (f_D - P_Q f_D) p^* \,\mathrm{dx} \qquad \text{since } \nabla\cdot\boldsymbol{u}_{h,T} = P_Q f_D \\
= &- \int_{\Omega_D} (f_D - P_Q f_D)(p^* - P_Q p^*) \,\mathrm{dx} \\
&\leq \|f_D - P_Q f_D\|_{\Omega_D} \|p^* - P_Q p^*\|_{\Omega_D} \preceq h^{s-1+r} \|f_D\|_{H^{s-1}(\Omega_D)} \|p^*\|_{H^r(\Omega_D)} \\
&\preceq h^{s-1+r} \|f_D\|_{H^{s-1}(\Omega_D)} \|\boldsymbol{u} - \boldsymbol{u}_{h,T}\|_{\Omega_S}.
\end{aligned}$$

The proof is concluded by combing the above estimates. □

3.3 L^2-Estimate in the Darcy Subdomain

Theorem 3 *Let the assumptions of Theorem 2 hold. Assume further that* $\boldsymbol{u}_D \in \boldsymbol{H}^s(\Omega_D)$ *for* $s \in [2, k+1]$. *Then, the following error estimate holds*

$$\|\boldsymbol{u} - \boldsymbol{u}_{h,T}\|_{\Omega_D} \preceq h^{s-1+r}(\|\boldsymbol{u}\|_{H^s(\Omega_S)} + \|\boldsymbol{u}\|_{H^s(\Omega_D)} + \|f_D\|_{H^{s-1}(\Omega_D)}). \tag{16}$$

We need the following Lemma to prove Theorem 3.

Lemma 5 *We have*

$$\|(\boldsymbol{u} - \boldsymbol{u}_{h,T}) \cdot \boldsymbol{n}\|_{H^{-1/2}(\Gamma_{SD})} \preceq h^{s-1+r}(\|\boldsymbol{u}\|_{H^s(\Omega_S)} + \|\boldsymbol{u}\|_{H^{s-1}(\Omega_D)} + \|f_D\|_{H^{s-1}(\Omega_D)}).$$

Moreover, there is a function $\boldsymbol{w} \in \boldsymbol{H}(\mathrm{div}; \Omega_D) \cap \boldsymbol{H}^{1/2}(\Omega_D)$ *satisfying* $\nabla\cdot\boldsymbol{w} = 0$ *on* Ω, $\boldsymbol{w} \cdot \boldsymbol{n} = 0$ *on* Γ_D, *and* $\boldsymbol{w} \cdot \boldsymbol{n} = (\boldsymbol{u} - \boldsymbol{u}_{h,T}) \cdot \boldsymbol{n}$ *on* Γ_{SD}, *such that*

$$\begin{aligned}
\|\boldsymbol{w}\|_{\Omega_D} &\preceq \|(\boldsymbol{u} - \boldsymbol{u}_{h,T}) \cdot \boldsymbol{n}\|_{H^{-1/2}(\Gamma_{SD})}, \\
\|\boldsymbol{w}\|_{\boldsymbol{H}^{1/2}(\Omega_D)} &\preceq \|(\boldsymbol{u} - \boldsymbol{u}_{h,T}) \cdot \boldsymbol{n}\|_{\Gamma_{SD}}.
\end{aligned}$$

Proof Since $\boldsymbol{u} - \boldsymbol{u}_{h,T} \in H(\text{div}; \Omega_S)$, its normal trace satisfies, c.f. [19],

$$\|(\boldsymbol{u} - \boldsymbol{u}_{h,T}) \cdot \boldsymbol{n}\|_{H^{-1/2}(\partial\Omega_S)} \preceq \|\boldsymbol{u} - \boldsymbol{u}_{h,T}\|_{\boldsymbol{H}(\text{div};\Omega_S)}.$$

Since $(\boldsymbol{u} - \boldsymbol{u}_{h,T}) \cdot \boldsymbol{n} = 0$ on Γ_S, following the approach [16], we have

$$\|(\boldsymbol{u} - \boldsymbol{u}_{h,T}) \cdot \boldsymbol{n}\|_{H^{-1/2}(\Gamma_{SD})} \preceq \|\boldsymbol{u} - \boldsymbol{u}_{h,T}\|_{\boldsymbol{H}(\text{div};\Omega_S)}.$$

Since $\nabla\cdot(\boldsymbol{u} - \boldsymbol{u}_{h,T}) = 0$ on Ω_S, we have with Theorem 2

$$\begin{aligned}\|\boldsymbol{u} - \boldsymbol{u}_{h,T}\|_{\boldsymbol{H}(\text{div};\Omega_S)} &= \|\boldsymbol{u} - \boldsymbol{u}_{h,T}\|_{\Omega_S} \\ &\preceq h^{s-1+r}(\|\boldsymbol{u}\|_{\boldsymbol{H}^s(\Omega_S)} + \|\boldsymbol{u}\|_{\boldsymbol{H}^{s-1}(\Omega_D)} + \|f_D\|_{H^{s-1}(\Omega_D)}).\end{aligned}$$

The other two inequalities are given in [20, Lemma 11]. □

Now, we are ready to prove Theorem 3.

Proof of Theorem 3

Let $\boldsymbol{w}$ be given by Lemma 5. Let $\boldsymbol{v}$ be such that $\boldsymbol{v} = 0$ on Ω_S, and $\boldsymbol{v} = \Pi_V\boldsymbol{u} - \boldsymbol{u}_{h,T} - \Pi_V\boldsymbol{w}$ on Ω_D. We have $\boldsymbol{v} \cdot \boldsymbol{n} = (\Pi_V\boldsymbol{u} - \boldsymbol{u}_{h,T} - \Pi_V\boldsymbol{w}) \cdot \boldsymbol{n} = 0$ on Γ_{SD}, hence $\boldsymbol{v} \in \boldsymbol{\Sigma}_h$ and $\nabla\cdot\boldsymbol{v} = 0$. Taking $\underline{\boldsymbol{v}}_h = (\boldsymbol{v}, 0)$ in Eq. (11a), we get

$$a_h(\underline{\boldsymbol{u}} - \underline{\boldsymbol{u}}_h, \underline{\boldsymbol{v}}_h) = \int_{\Omega_D} K^{-1}(\boldsymbol{u} - \boldsymbol{u}_{h,T})(\Pi_V\boldsymbol{u} - \boldsymbol{u}_{h,T} - \Pi_V\boldsymbol{w})\,\text{dx} = 0.$$

This implies that

$$\begin{aligned}\|\boldsymbol{u} - \boldsymbol{u}_{h,T}\|_{\Omega_D} &\leq \|\boldsymbol{u} - \Pi_V\boldsymbol{u} - \Pi_V\boldsymbol{w}\|_{\Omega_D} \\ &\preceq \|\boldsymbol{u} - \Pi_V\boldsymbol{u}\|_{\Omega_D} + \|\Pi_V\boldsymbol{w}\|_{\Omega_D} \\ &\preceq h^s\|\boldsymbol{u}\|_{\boldsymbol{H}^s(\Omega_D)} + \|(\boldsymbol{u} - \boldsymbol{u}_{h,T}) \cdot \boldsymbol{n}\|_{H^{-1/2}(\Gamma_{SD})} \\ &\preceq h^s\|\boldsymbol{u}\|_{\boldsymbol{H}^s(\Omega_D)} + h^{s-1+r}\left(\|\boldsymbol{u}\|_{\boldsymbol{H}^s(\Omega_S)} + \|\boldsymbol{u}\|_{\boldsymbol{H}^{s-1}(\Omega_D)} + \|f_D\|_{H^{s-1}(\Omega_D)}\right).\end{aligned}$$

□

4 Numerical Results

In this section, we present numerical results in two dimensions to verify the theoretical findings in Sect. 3. The numerical results are performed using the NGSolve software [35].

We consider an example with a smooth manufactured exact solution constructed in [12]. The domain is a unit square $\Omega = [0, 1] \times [0, 1]$ with the Darcy subdomain $\Omega_D = [0, 1] \times [0, 0.5]$, and Stokes subdomain $\Omega_S = [0, 1] \times [0.5, 1]$. We take $\nu = K = 1$, and $\gamma = (1 + 4\pi^2)/2$. The source terms are chosen such that the problem has the exact solution:

$$\boldsymbol{u}_S(x, y) = \begin{bmatrix} -1/(2\pi^2)\sin(\pi x)\exp(y/2) \\ 1/\pi\cos(\pi x)\exp(y/2) \end{bmatrix}, \qquad p_S(x, y) = -1/\pi\cos(\pi x)\exp(y/2),$$

$$\boldsymbol{u}_D(x, y) = \begin{bmatrix} -2\sin(\pi x)\exp(y/2) \\ 1/\pi\cos(\pi x)\exp(y/2) \end{bmatrix}, \qquad p_D(x, y) = -2/\pi\cos(\pi x)\exp(y/2).$$

We apply the numerical scheme (5) using polynomial degree k for the velocity space $\boldsymbol{\Sigma}_h$, $k - 1$ for the pressure space Q_h, and $k - 1$ for the facet tangential velocity space M_h with

Table 1 History of convergence of the L^2-velocity errors

k	k_f	Mesh	$\|\boldsymbol{u}_S - \boldsymbol{u}_{h,T}\|_{\Omega_S}$		$\|\boldsymbol{u}_D - \boldsymbol{u}_{h,T}\|_{\Omega_D}$		$\|\nabla\cdot\boldsymbol{u}_{h,T} - \chi_D P_Q f_D\|_\Omega$
		h	Error	Order	Error	Order	
1	0	1/4	1.197E−2	–	5.165E−2	–	1.297E−15
		1/8	2.238E−3	2.43	1.069E−2	2.25	3.434E−15
		1/16	4.792E−4	2.29	2.834E−3	1.94	5.939E−15
		1/32	1.106E−4	2.14	6.932E−4	2.03	1.278E−14
		1/64	2.745E−5	2.04	1.735E−4	2.01	2.680E−14
2	1	1/4	5.166E−4	–	4.491E−3	–	1.094E−15
		1/8	4.121E−5	3.65	3.745E−4	3.58	3.447E−15
		1/16	4.504E−6	3.19	5.148E−5	2.86	6.185E−15
		1/32	4.876E−7	3.21	5.678E−6	3.18	1.248E−14
		1/64	6.145E−8	2.99	6.853E−7	3.05	2.732E−14
3	2	1/4	4.088E−5	–	1.306E−4	–	1.192E−15
		1/8	1.590E−6	4.68	3.851E−6	5.08	3.788E−15
		1/16	6.681E−8	4.57	2.269E−7	4.09	6.525E−15
		1/32	3.383E−9	4.30	1.236E−8	4.20	1.228E−14
		1/64	2.023E−10	4.06	7.3410E−10	4.07	2.679E−14
4	3	1/4	1.554E−6	–	1.087E−5	–	1.669E−15
		1/8	2.485E−8	5.97	1.997E−7	5.77	3.435E−15
		1/16	5.914E−10	5.39	6.334E−9	4.98	6.792E−15
		1/32	1.485E−11	5.32	1.602E−10	5.31	1.253E−14
		1/64	9.610E−13	3.95	1.215E−11	3.72	2.693E−14

k varying from 1 to 4. For all the tests, we take the stabilization parameter $\alpha = 10\,k^2$. The history of convergence for the L^2-error of the velocity in each subdomain and the L^2 norm of the quantity $\nabla\cdot\boldsymbol{u}_{h,T} - \chi_D P_Q f_D$ are recorded in Table 1. We observe optimal order of convergence $k+1$ for each error. This result is in full agreement with our main results in Theorems 2 and 3 for $k \geq 2$. However, our analysis could not explain the optimal convergence for the lowest-order case ($k = 1$), since the analysis requires the facet tangential velocity space to include polynomials of degree 1, see Lemma 1. The optimal convergence of this lowest order case requires further investigation. We also observe the strong mass conservation result, c.f. Remark 1, that the quantity $\nabla\cdot\boldsymbol{u}_{h,T} - \chi_D P_Q f_D$ is machine zero for all the tests.

Finally, we remark that, if we increase the polynomial degree of the facet tangential velocity space to be k, similar error and convergence rates were obtained in our numerical results not recorded here.

Hence, this modification is less attractive to the method tested here as it gives similar accuracy but has a lot more globally coupled degrees of freedom, see also the performance comparisons for vector-Laplace and Stokes problems with similar discretizations in [25, Section 4.3] and [23, Section 5.2].

5 Conclusion

We presented a new finite element method for the coupling of Stokes and Darcy flow, where the Stokes flow is discretized by a divergence-conforming HDG method, and the Darcy flow by a mixed finite element method. Exact mass conservation is guaranteed. We presented optimal error estimates of the proposed method with numerical results supporting the theoretical findings.

References

1. Arbogast, T., Brunson, D.S.: A computational method for approximating a Darcy–Stokes system governing a vuggy porous medium. Comput. Geosci. **11**, 207–218 (2007)
2. Beavers, G.S., Joseph, D.D.: Boundary conditions at a naturally impermeable wall. J. Fluid Mech. **20**, 197–207 (1967)
3. Bernardi, C., Hecht, F., Pironneau, O.: Coupling Darcy and Stokes equations for porous media with cracks. M2AN Math. Model. Numer. Anal. **39**, 7–35 (2005)
4. Bernardi, C., Rebollo, T.C., Hecht, F., Mghazli, Z.: Mortar finite element discretization of a model coupling Darcy and Stokes equations. M2AN Math. Model. Numer. Anal. **42**, 375–410 (2008)
5. Boffi, D., Brezzi, F., Fortin, M.: Mixed Finite Element Methods and Applications, vol. 44 of Springer Series in Computational Mathematics. Springer, Heidelberg (2013)
6. Brenner, S.C.: Korn's inequalities for piecewise H^1 vector fields. Math. Comput. **73**, 1067–1087 (2004)
7. Burman, E., Hansbo, P.: Stabilized Crouzeix–Raviart element for the Darcy-Stokes problem. Numer. Methods Partial Differ. Eqs. **21**, 986–997 (2005)
8. Burman, E., Hansbo, P.: A unified stabilized method for Stokes and Darcy's equations. J. Comput. Appl. Math. **198**, 35–51 (2007)
9. Cockburn, B., Sayas, F.-J.: Divergence-conforming HDG methods for Stokes flow. Math. Comput. **83**, 1571–1598 (2014)
10. Cockburn, B., Kanschat, G., Schötzau, D.: A locally conservative LDG method for the incompressible Navier–Stokes equations. Math. Comput. **74**, 1067–1095 (2005)
11. Cockburn, B., Kanschat, G., Schötzau, D.: A note on discontinuous Galerkin divergence-free solutions of the Navier–Stokes equations. J. Sci. Comput. **31**, 61–73 (2007)
12. Correa, M., Loula, A.: A unified mixed formulation naturally coupling Stokes and Darcy flows. Comput. Methods Appl. Mech. Eng. **198**, 2710–2722 (2009)
13. Discacciati, M., Miglio, E., Quarteroni, A.: Mathematical and numerical models for coupling surface and groundwater flows. Appl. Numer. Math. **43**, 57–74 (2002). 19th Dundee Biennial Conference on Numerical Analysis (2001)
14. Ervin, V.J., Jenkins, E.W., Sun, S.: Coupled generalized nonlinear Stokes flow with flow through a porous medium. SIAM J. Numer. Anal. **47**, 929–952 (2009)
15. Fu, G., Jin, Y., Qiu, W.: Parameter-free superconvergent h(div)-conforming HDG methods for the brinkman equations. arXiv preprint arXiv:1607.07662 (2016)
16. Galvis, J., Sarkis, M.: Non-matching mortar discretization analysis for the coupling Stokes–Darcy equations. Electron. Trans. Numer. Anal. **26**, 350–384 (2007)
17. Gatica, G.N., Meddahi, S., Oyarzúa, R.: A conforming mixed finite-element method for the coupling of fluid flow with porous media flow. IMA J. Numer. Anal. **29**, 86–108 (2009)
18. Gatica, G.N., Oyarzúa, R., Sayas, F.-J.: Convergence of a family of Galerkin discretizations for the Stokes–Darcy coupled problem. Numer. Methods Partial Differ. Eqs. **27**, 721–748 (2011)
19. Girault, V., Raviart, P.-A.: Finite Element Methods for Navier–Stokes Equations. Springer, Berlin (1986)
20. Girault, V., Kanschat, G., Rivière, B.: Error analysis for a monolithic discretization of coupled Darcy and Stokes problems. J. Numer. Math. **22**, 109–142 (2014)
21. Kanschat, G., Rivière, B.: A strongly conservative finite element method for the coupling of Stokes and Darcy flow. J. Comput. Phys. **229**, 5933–5943 (2010)
22. Layton, W.J., Schieweck, F., Yotov, I.: Coupling fluid flow with porous media flow. SIAM J. Numer. Anal. **40**(2002), 2195–2218 (2003)
23. Lederer, P.L., Lehrenfeld, C., Schöberl, J.: Hybrid discontinuous Galerkin methods with relaxed h(div)-conformity for incompressible flows. Part I. arXiv preprint arXiv:1707.02782 (2017)
24. Lehrenfeld, C.: Hybrid discontinuous Galerkin methods for solving incompressible flow problems. Diploma Thesis, MathCCES/IGPM, RWTH Aachen (2010)

25. Lehrenfeld, C., Schöberl, J.: High order exactly divergence-free hybrid discontinuous Galerkin methods for unsteady incompressible flows. Comput. Methods Appl. Mech. Eng. **307**, 339–361 (2016)
26. Linke, A.: On the role of the Helmholtz decomposition in mixed methods for incompressible flows and a new variational crime. Comput. Methods Appl. Mech. Eng. **268**, 782–800 (2014)
27. Nassehi, V.: Modelling of combined NavierStokes and Darcy flows in crossflow membrane filtration. Chem. Eng. Sci. **53**, 1253–1265 (1998)
28. Nassehi, V., Waghode, A.N., Hanspal, N.S., Wakeman, R.J.: Mathematical modelling of flow through pleated cartridge filters. In: Progress in industrial mathematics at ECMI 2004, vol. 8 of Mathematics in Industry, pp. 298–302. Springer, Berlin (2006)
29. Oikawa, I.: A hybridized discontinuous Galerkin method with reduced stabilization. J. Sci. Comput. **65**, 327–340 (2015)
30. Qiu, W., Shen, J., Shi, K.: An HDG method for linear elasticity with strong symmetric stresses. Math. Comput. **87**, 69–93 (2018)
31. Rivière, B.: Analysis of a discontinuous finite element method for the coupled Stokes and Darcy problems. J. Sci. Comput. **22**(23), 479–500 (2005)
32. Rivière, B., Yotov, I.: Locally conservative coupling of Stokes and Darcy flows. SIAM J. Numer. Anal. **42**, 1959–1977 (2005)
33. Rui, H., Zhang, R.: A unified stabilized mixed finite element method for coupling Stokes and Darcy flows. Comput. Methods Appl. Mech. Eng. **198**, 2692–2699 (2009)
34. Saffman, P.: On the boundary condition at the surface of a porous media. Stud. Appl. Math. **50**, 292–315 (1971)
35. Schöberl, J.: C++11 Implementation of Finite Elements in NGSolve, ASC Report 30/2014, Institute for Analysis and Scientific Computing, Vienna University of Technology (2014)
36. Schroeder, P.W., Linke, A., Lehrenfeld, C., Lube, G.: Towards computable flows and robust estimates for inf-sup stable fem applied to the time-dependent incompressible Navier–Stokes equations. arXiv preprint arXiv:1709.03063 (2017)
37. Urquiza, J.M., N'Dri, D., Garon, A., Delfour, M.C.: Coupling Stokes and Darcy equations. Appl. Numer. Math. **58**, 525–538 (2008)
38. Warburton, T., Hesthaven, J.S.: On the constants in hp-finite element trace inverse inequalities. Comput. Methods Appl. Mech. Eng. **192**, 2765–2773 (2003)
39. Xie, X., Xu, J., Xue, G.: Uniformly-stable finite element methods for Darcy–Stokes–Brinkman models. J. Comput. Math. **26**, 437–455 (2008)